Network pharmacological analysis of active components of Tongqiao Huoxue Decoction in the treatment of intracerebral hemorrhage

Ji Wu[1,2#], Xue-Yu Li[1,2#], Jing Liang[3#], Jian Xie[4], Cheng-Neng Deng[4], Zhi-Jun Chen[4], Chang-Sheng Lai[2,4], Zhao-Jian Yang[2,4]

[1]Department of Neurosurgery, Affiliated Hospital of Youjiang Medical University for Nationalities, Baise, China; [2]Clinical College of Youjiang Medical University for Nationalities, Baise, China; [3]Department of Pediatrics, The Second Affiliated Hospital of Xinjiang Medical University, Urumchi, China; [4]Department of Neurosurgery, The Red Cross Hospital of Yulin City, Yulin, China

Contributions: (I) Conception and design: J Wu, XY Li, J Liang; (II) Administrative support: ZJ Yang; (III) Provision of study materials or patients: J Wu; (IV) Collection and assembly of data: J Wu, ZJ Yang; (V) Data analysis and interpretation: XY Li, J Liang; (VI) Manuscript writing: All authors; (VII) Final approval of manuscript: All authors.

[#]These authors contributed equally to this work.

Correspondence to: Zhao-Jian Yang. Department of Neurosurgery, The Red Cross Hospital of Yulin City, Yulin, China. Email: Y5330838@163.com.

Background: Intracerebral hemorrhage (ICH) is a type of stroke which results in a high disability and mortality rate and has a poor prognosis. Tongqiao Huoxue Decoction (TQHXD) is a classical Chinese prescription. Clinical practice has proven that TQHXD can promote blood circulation and can effectively treat ICH and its sequelae. However, the current mechanism is still unclear.

Methods: The chemical components and target genes of TQHXD were collected from the Traditional Chinese medicine (TCM) Systems Pharmacology and Bioinformatics Analysis Tool for Molecular Mechanism of Traditional Chinese Medicine analysis platforms, and the gene expression data of ICH tissues were downloaded from the Gene Expression Omnibus (GEO) database. Weighted gene co-expression network analysis (WGCNA) was performed to obtain differentially co-expressed gene pairs and build a drug-target-disease network. Gene Ontology (GO) and Kyoto Encyclopedia of Genes and Genomes (KEGG) enrichment analyses were performed on the obtained target genes and shared genes. Finally, molecular docking was carried out to further clarify the utility of TQHXD for the treatment of ICH.

Results: A total of 304 differentially expressed genes in ICH, 42 TQHXD active ingredients, and 279 predicted targets of its active compounds were obtained. Bioinformatics analysis showed that they were involved in angiogenesis, the regulation of wound healing, and other biological processes. Furthermore, their participation in fluid shear stress and the atherosclerosis signaling pathway indicated their close association with the pathological processes of ICH. Finally, molecular docking was carried out to further confirm the tightly binding structural sites of the effective components of TQHXD and key proteins.

Conclusions: In summary, the results of this study suggest that the mechanism of action of TQHXD in the treatment of ICH involves multiple targets and signaling pathways related to its occurrence and development. This study not only provides a new theoretical basis for the treatment of ICH with traditional Chinese medicine, but also provides new ideas for the research and development of drugs for the treatment of ICH.

Keywords: Network pharmacology; Tongqiao Huoxue Decoction (TQHXD); intracerebral hemorrhage (ICH); blood-brain barrier (BBB); traditional Chinese medicine

Submitted Feb 28, 2022. Accepted for publication Apr 13, 2022.

doi: 10.21037/atm-22-1403

View this article at: https://dx.doi.org/10.21037/atm-22-1403

Introduction

Intracerebral hemorrhage (ICH) refers to hemorrhage within the brain parenchyma. It is a common stroke type and the main manifestations are neurological deterioration and poor prognosis. Although ICH has a lower incidence than ischemic stroke, it may reach 50% due to short-term mortality (1,2). Due to the high mortality rate of ICH, it has now become a major issue worldwide. After active treatment, more than 20% of ICH patients have neurological dysfunction of varying degrees and still need long-term rehabilitation (3).

ICH is prone to recurrence. The mid-term and long-term mortality and functional outcomes after ICH are greatly affected by the occurrence of major vascular events. The spontaneous recurrence rate of ICH in survivors is 1.8–7.4% in the first year and 2.0–2.4% thereafter (4). In recent years, progress has been made in research on the pathogenesis of ICH. For example, oxidative stress plays an important role after the onset of ICH, which can lead to irreversible destruction of the gray matter of the neurovascular unit (NVU), dysfunction of the blood-brain barrier (BBB), the occurrence of fatal brain edema, and the death of brain cells (5). In addition, various substances in the blood also increase the incidence of bleeding, among which a high concentration of neurotoxins can directly kill neurons, leading to poor prognosis. However, the neuroinflammatory cascade triggered by the immune response after ICH further aggravates neurological damage. It has been demonstrated that pathophysiological changes in the NVU and glial network after ICH provide therapeutic targets for ameliorating ICH-induced secondary brain injury (6-8).

These studies help provide a theoretical basis for cell-targeted drug therapy for ICH, but the current treatment of ICH is mainly aimed at controlling the growth of hematomas in the acute phase, reducing blood pressure to 140 mmHg or lower, and using tranexamic acid (TXA) and other hemostatic drugs for treatment (9,10). Because most patients miss the optimal treatment time, the treatment effect is often unsatisfactory. Moreover, these drugs have many clinical side effects. Some newly discovered drugs are currently in clinical trials, and large-scale clinical research and comprehensive marketing have not been carried out.

Traditional Chinese medicine (TCM) mainly uses a holistic view and syndrome differentiation as the leading ideas of clinical practice. It is widely used in the treatment of diseases (11). Clinical studies have shown that in the acute and remission phase of ICH, TCM can promote the absorption of the hematoma and improve the symptoms caused by ICH. Tongqiao Huoxue Decoction (TQHXD) was created by Wang Qingren of the Qing Dynasty. It is composed of musk, red peony root, Chuanxiong, peach kernel, safflower, and other medicines. In China, TQHXD has been widely used in brain trauma syndrome, dizziness, and emotional disorders caused by ICH (12). Recent studies have shown that TQHXD can participate in the treatment of stroke through various mechanisms. For example, the drug can induce platelet aggregation and prolong coagulation time by regulating the permeability of the BBB (13-15), but the key targets and signaling pathways of TQHXD in the treatment of ICH are still unclear and need to be further studied. In the search for differentially related genes of spontaneous ICH, we used sequencing data of human brain tissues with spontaneous ICH to find the differentially related genes of normal brain tissues and bleeding brain tissues. For drugs and considering the relationship between drugs and BBB, we found the active ingredient of QTHXD that can pass the BBB. Systems biology and network pharmacology can be used to construct a complex network between drug-target-disease, and network analysis theory can be used to study drug action mechanisms from a holistic perspective. Network pharmacology can be used to predict the relevant components, targets, and pathways of TQHXD in ICH intervention, and to explore the overall regulation of drugs on ICH. We found that TQHXD accelerates the recovery of ICH by regulating coagulation, accelerating the migration of vascular endothelial cells to the ruptured vessel and promoting the sprouting of new blood vessels and wound healing. Therefore, these findings provide new ideas for future research. We present the following article in accordance with the STREGA reporting checklist (available at https://atm.amegroups.com/article/view/10.21037/atm-22-1403/rc).

Methods

Search for TQHXD active components

The active ingredients of TQHXD were downloaded from the TCM Systems Pharmacology (TCMSP) (https://old.tcmsp-e.com/tcmsp.php) and BATMAN-TCM databases (http://bionet.ncpsb.org.cn/batman-tcm/index.php) (16,17). TCMSP contains many Chinese medicine

entries and drug target networks, from which a large amount of herbal information can be obtained, including drug composition, drug similarity (DL), human oral bioavailability (OB), molecular name, molecular weight (MW), half-life (HL), BBB, and other important Chinese medicine monomer information. OB is the most important pharmacokinetic property of oral drugs, which is used to evaluate the delivery efficiency of drugs to the systemic circulation. Drug-like properties are used to evaluate the possibility of a compound becoming a drug, and only molecules with higher OB and DL may have good pharmacological activity. With reference to the Drug Bank database, the average DL value of a drug is 0.18. A study has shown that compounds with BBB <–0.3 are considered non-penetrating (BBB–), moderate penetration (BBB±) is defined as BBB from –0.3 to 0.3, and strong penetration (BBB) is defined as BBB from 0.3 to 0.3 (18). Therefore, the OB standard defines ingredients with ≥30%, DL ≥0.18, and BBB >–0.3 as effective ingredients. In addition, musk and other ingredients could not be found in the TCMSP database. The BATMAN-TCM analysis platform was used to search for the ingredients and composition targets of musk. BATMAN-TCM is an online analysis tool for TCM molecular bioinformatics. It includes the prediction of TCM components and component targets. According to the prediction score of drug-target interaction prediction, the "score cut-off" value was set to 20 and the P value was set to 0.05 to obtain the final potential target (19). We obtained 42 kinds of effective active ingredients that can pass the BBB, of which musk, safflower, jujube, red peony, and Chuanxiong, among others, accounted for 88% of the total pharmaceutical ingredients.

Identification of targets of active ingredients

After screening the active ingredients of TQHXD through the TCMSP database and the BATMAN-TCM database, the ingredients were uploaded to the PubChem database (https://www.ncbi.nlm.nih.gov/) (20). The Uniprot database (https://www.uniprot.org/) (21) was used to standardize the predicted target, and the target of musk's drug is: score the top ten by setting the "score cutoff" value greater than 20 in the BATMAN-TCM database, and adding the TCMSP database. The intersection of the data obtained with the BATMAN-TCM database was regarded as the final gene target of TQHXD. We finally obtained 279 drug targets, of which musk had 202 targets.

ICH-related gene screening

The study was conducted in accordance with the Declaration of Helsinki (as revised in 2013). All data was obtained from the Gene Expression Omnibus (GEO) database, which is publicly available (22). We searched the database with "ICH" as the keyword, and obtained the dataset of GSE24265, which mainly included the data of 4 ICH cases. The peripheral hematoma area was used for the disease group, while the gray and white matter on the contralateral side were used as the control. The standardization of the data and the screening of differentially expressed genes (DEGs) were performed using the limma software package (version 3.5.1) of R language. DEGs were identified in ICH patient samples compared with control samples. In order to identify genes with significant differences in expression fold change (FC), we set the screening criteria to screen genes with FC value (|log2FC|) >2 and P value <0.05.

The weighted gene co-expression network analysis (WGCNA) Bioconductor package is a collection of functions developed by Langfelder *et al.* to realize WGCNA, including soft power selection, GCMs (Gene Characteristic Modules) recognition, and module visualization, among others (23,24). In short, the soft threshold that could reach a relatively high scale-free network topology was selected, that is, the lowest power, and then the blockwisemodules function was used to identify the GCM. The minimum and maximum number of genes contained in a GCM were set to 50 and 500, respectively. The characteristic gene, the first principal component of a specific GCM, was used to indicate the overall expression of GCM. In addition, 2 parameters representing the correlation between a specific gene expression value and a characteristic gene or clinical trait were used to evaluate the importance of genes. Module membership (MM) calculated the Pearson correlation coefficient of the gene and the characteristic gene expression value. The Pearson correlation coefficient between the gene expression value of interest and the clinical feature was calculated to represent Gene Significance (GS). Therefore, the higher the MM and GS, the closer the relationship between the gene and clinical characteristics. In this study, the normalized read count of all genes was used for WGCNA to identify important GCMs and core genes related to ICH. In addition, the correlation between GCM and ICH was evaluated by calculating the Pearson correlation coefficient of each GCMs characteristic gene

and ICH Finally, we merged the core genes obtained by WGCNA with DEGs to finally obtain 304 DEGs of ICH.

Construction of the drug-gene targeting network

By using Cytoscape software (v.3.8.0) to construct the 279 target gene networks of the active ingredients of TCM that pass through the BBB, the target of 11 genes and the network of compound-target-disease (CTD) same drug-disease network, the TQHXD active ingredient network, molecular targets, and CTD network core relationship could be observed. The CytoNCA plug-in was used to calculate the node information of each node. The node that exceeded the average value of all nodes in the network was the key effective component and key candidate target. The score value of the node reflected the strength of the node and its neighbors. The greater the strength of the node and its neighbors, the more important its role in the network.

Protein-protein interaction (PPI) analysis

The above-mentioned 279 drug target genes and 19 drug-disease genes were imported into the STRING database to construct a PPI network (25). We set a confidence score of minimum required interaction score greater than or equal to 0.7 to select the core PPI target and construct a PPI network. Then, Cytoscape was applied to examine the potential correlations between these genes. The target-to-target (TT) network between TQHXD and ICH was constructed using Cytoscape's plug-in CytoNCA. The TQHXD and ICH intersection gene protein interaction network was constructed using Cytoscape's plug-in BisoGenet and visualized using Cytoscape (26-28).

Gene Ontology (GO) and Kyoto Encyclopedia of Genes and Genomes (KEGG) pathway analysis

To further clarify the biological effects of the active ingredients of TQHXD and the potential mechanism of the therapeutic effects on ICH, GO and KEGG analyses were performed. R software was used to process the above-mentioned 279 drug genes, 304 disease genes, and 11 drug-disease intersection genes, and R software's clusterProfiler, org.Hs.eg.db, enrichplot, ggplot2, and other packages (version 3.6.2) were used to visualize GO and KEGG enriched pathways. The P value filter condition was pvalueFilter <0.05, and the corrected P value filter condition was qvalueFilter <0.05.

Molecular docking

The 2D structures of the active ingredients of TQHXD and the main target of ICH were downloaded from the PubChem (https://pubchem.ncbi.nlm.nih.gov/) and Protein Data Bank (PDB) databases (http://www.rcsb.org/) (29,30), then AutoDOCK software was used to complete the docking analysis of the main target and the corresponding small molecule drug (31). Their binding energy was visualized with a heat map. The lower the binding energy, the better the docking effect. Finally, MOE software (v.2019.0102) was used to verify the molecular docking of the molecular pair with the lowest binding energy between the small drug molecule and the protein macromolecule (32) to determine their good interaction sites.

Analysis of core molecule docking gene enrichment analysis

The Cytoscape plug-in ClueGO was used to analyze and visualize the biological process of constructing the core genes in the CTD network and combine the results of KEGG pathway enrichment and molecular docking of the previous shared genes to jointly explain the possible mechanism of TQHXD in the treatment of ICH.

Statistical analysis

All statistical analyses were conducted using R software (version 4.1.0). Differential gene analysis was performed using the limma package. The following threshold was set: |logFC| >2 and P value <0.05. P value <0.05 indicated a statistically significant difference.

Results

This study can be divided into 4 parts in order. *Figure 1* shows the whole process of the analysis. First, the chemical components of TQHXD and the target genes were collected from the TCSMP and BATMAN-TCM analysis platforms. Then, the GSE24265 dataset (the gene expression data of the brain tissue of patients with ICH) was downloaded from the GEO database, and WGCNA was performed to obtain the DEG pairs. Next, the Chinese medicine-related network and the ICH gene network were merged together, and topological analysis was performed to filter out the required core network. Finally, GO

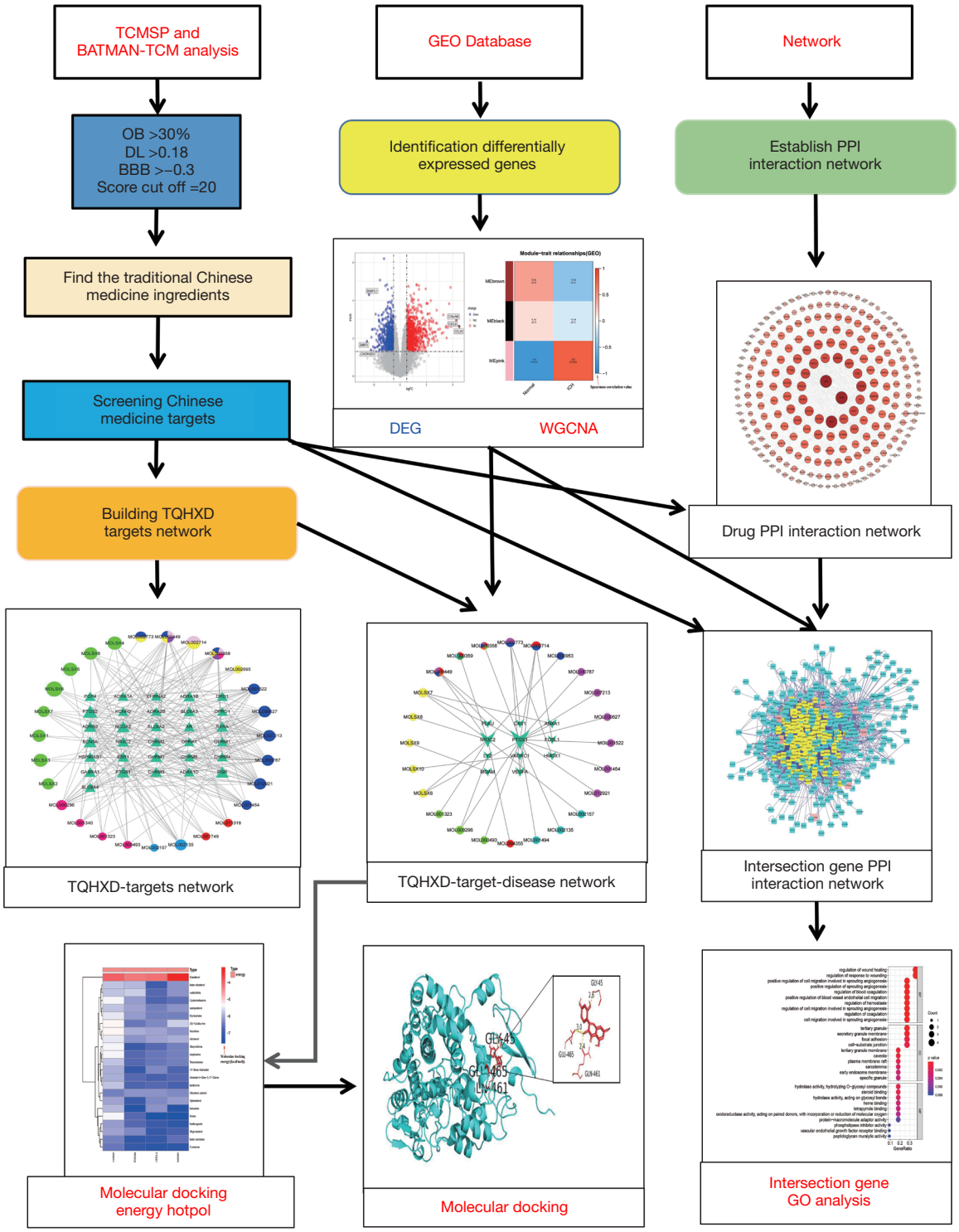

Figure 1 Flow chart of the systematic analysis of TQHXD for ICH treatment. TCMSP, Traditional Chinese Medicine Systems Pharmacology Database and Analysis Platform; OB, oral bioavailability; DL, drug-likeness; BBB, blood-brain barrier; GEO, gene expression omnibus; PPI, protein-protein interaction; TQHXD, Tongqiao Huoxue Decoction; DEG, differentially expressed gene; WGCNA, weighted gene co-expression network analysis; ICH, intracerebral hemorrhage; GO, Gene Ontology.

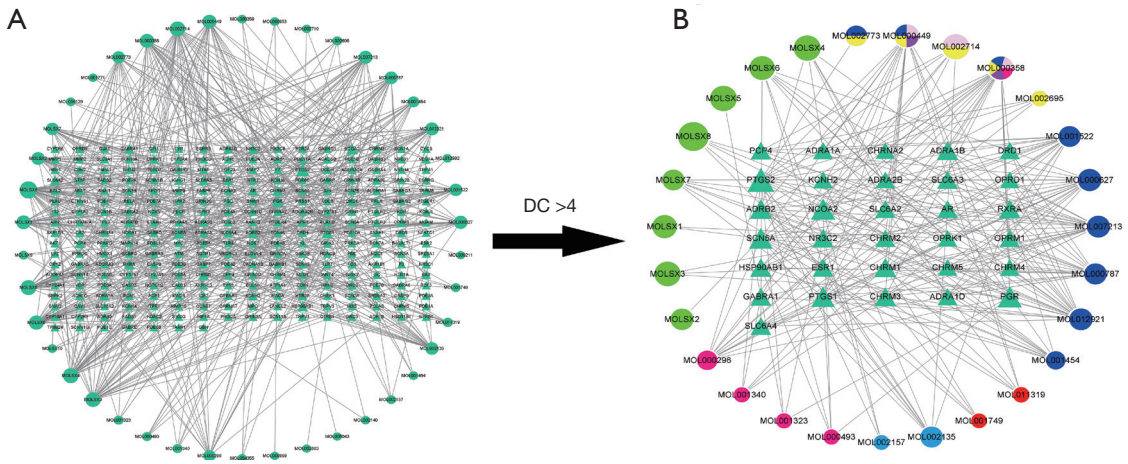

Figure 2 TQHXD active ingredient network and its molecular targeting relationship. (A) TQHXD formulae network of all active components and molecular targeting network (drug nodes are round, molecular nodes are triangular). (B) The 27 drug nodes (round nodes; musk is green, peach kernel is pink, Chuanxiong is sky blue, green onion is red, Dazao is dark blue, Honghua is yellow, and multiple drugs are mixed colors) and 31 molecular nodes (triangles). TQHXD, Tongqiao Huoxue Decoction; DC, degree centrality.

and KEGG analysis were performed on these targets to determine the mechanism of action of TQHXD in the treatment of ICH, as well as the molecular docking of core genes and TQHXD.

The formula of TQHXD and the screening of its active ingredients and targets

There are 8 TQHXD ingredients, namely musk, safflower, jujube, red peony, Chuanxiong, peach kernel, green onion, and ginger. In order to reveal the mechanism of TQHXD in the brain and in the treatment of ICH, our screening conditions were as follows: the OB standard was ≥30%, DL ≥0.18, and BBB >–0.3. The drug components of TQHXD were downloaded from the TCMIP and BATMAN-TCM analysis platforms, and the components were analyzed to construct a drug-target network. This initial network contained a total of 321 nodes and 593 edges. Then, using the PubChem database to screen the final effective ingredients, a total of 42 TCM ingredients were obtained, among which jujube occupied 11, musk occupied 10, Chishao and Honghua each occupied 8, and these 4 kinds of TCM accounted for 88.09% of the total ingredients. TQHXD yielded a total of 279 targets, of which musk accounted for 202, comprising 72.4% of the total targets.

Then, topology analysis was performed to filter out the required core network, which contained a total of 58 nodes and 237 edges. There were 27 drug nodes (round nodes; musk was green, peach kernels were pink, Chuanxiong was sky blue, green onions were red, Dazao was dark blue, Honghua was yellow, and multiple drugs were mixed colors) and 31 molecular node points (triangular nodes, the size of the area was proportional to the importance). Finally, the core target network was obtained through Cytoscape software (*Figure 2*).

Identification of DEGs in ICH

The expression data of ICH patient tissues was downloaded from the GEO database, and the limma package of R software was used to screen the downloaded data for DEGs. Compared with the brain tissue samples on the opposite side of the ICH, there were a total of 449 genes in the tissue from the hemorrhage area. The results showed that there were 318 up-regulated genes and 131 down-regulated genes. According to multiple changes, interleukin-8 (*CXCL8*), interleukin-20 (*CXCL20*), and *C15orf48* (belonging to the complex I NDUFA4 subunit family) were the top 3 genes with the highest degree of up-regulation, while zinc and ring finger 3 (*ZNRF3*), PWWP domain-containing protein (*MUM1L1*), and voltage-dependent calcium channel subunit alpha-2/delta-3 (*CACNA2D3*) were the top 3 most down-regulated genes (screening criteria: $P<0.05$, $|\log FC\text{filter}|>1$). A volcano plot and heat map (*Figure 3*) were created using the limma package to visualize the results of DEGs.

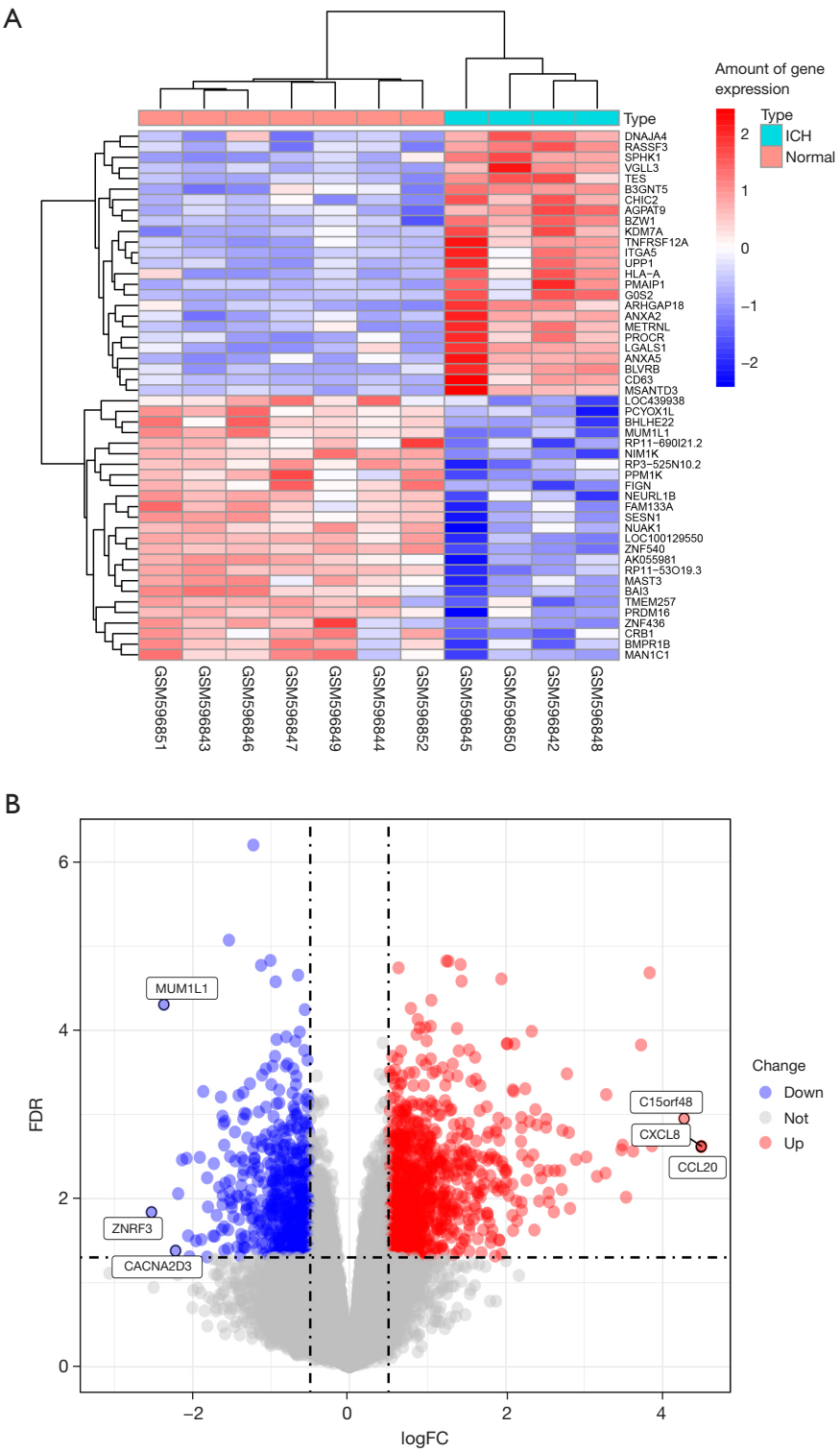

Figure 3 DEGs in ICH. (A) Heat maps of the top 50 DEGs in ICH (the ordinate value is the ratio multiple of ICH and normal tissue expression); (B) the DEGs volcano plot in ICH. DEGs, differentially expressed genes; ICH, intracerebral hemorrhage; FDR, false discovery rate; FC, fold change.

Then, the WGCNA Bioconductor package was used to perform WGCNA on the above expression data, and finally 8 Clustering_modules and 4 Module_traits were obtained. Among them, the correlation between the expression of the pink module and the cerebral hematoma area was 0.8 (P=0.003), and in this module there were 784 co-expressed genes. Finally, the co-expressed genes and DEGs were analyzed, and we found 304 common genes (*Figure 4*).

PPI network construction and analysis of drugs and diseases

First, the PPI network was constructed for the obtained TQHXD drug target. Because these components can enter the cerebrospinal fluid through the BBB, they can play an important role in the brain. We obtained a total of 279 targeted genes and networks for the effective components of TCM formulations. The graph included a total of 262 nodes and 1,204 edges. The core network was obtained through screening, which included 53 nodes and 313 edges (*Figure 5*). Among them, *TP53*, *JUN*, *MYC*, *AR*, *AKT1*, *NR3C1*, *VEGFA*, *MAPK14*, and other genes were the core genes of the network.

We then used the TQHXD drug target gene network obtained above and the DEGs of ICH to construct a drug-disease-target network. As shown in *Figure 6* in the network diagram, it was found that there was a one-to-one correspondence between 24 drug components and 11 drug-disease common genes in TQHXD. The network diagram included a total of 35 nodes and 34 edges. Among them, *PTGS1* was connected to 14 core drugs, and *NR3C2* was connected to 9 core drugs. In the figure, the active ingredients and targets of TQHXD and disease targets were interconnected to form a complex network, revealing that TQHXD can directly or indirectly act on multiple targets of ICH, thus exerting its therapeutic effects. Multiple targets play an effective therapeutic role. Furthermore, we also used the common 11 target networks of TQHXD and ICH to predict the PPI network, and used the CytoNCA plug-in in Cytoscape to confirm the core targets. A complex network (526 nodes and 4,793 edges) was obtained. The selection criteria were set as follows: betweenness >18; closeness >0.477; degree >11; eigenvector >0.095; local average connectivity (LAC) >6.8; network >8.5 (*Figure 7*). Finally, a core network with 65 nodes and 847 edges was selected.

GO and KEGG analysis of TQHXD targets and ICH differential genes

We further carried out GO and KEGG enrichment analysis on 304 genes of ICH, 279 targets of TQHXD, and 11 common targets using R software (*Figure 8*). The specific results of GO functional enrichment included the analysis of molecular function, biological process, and cellular component. GO analysis revealed that 279 targets were involved in a number of biological processes such as the G protein-couple receptor signaling pathway, coupled to cyclic nucleotide second messenger, vascular process in circulatory system, and regulation of blood vessel diameter. In addition, GO analysis of the 169 targets indicated that they were widely distributed and were mainly composed of ion channel complex, transmembrane transporter complex, and postsynaptic membrane. In terms of cell components, the main components were ion channel activity, neurotransmitter receptor activity, and extracellular ligand-ion channel activity.

The 304 DEGs of ICH were found to be involved in multiple biological processes. The main ones were neutrophil activation involved in immune response, leukocyte chemotaxis, and granulocyte migration. Cell components were mainly in secretory granule membrane and secretory cytoplasmic vesicle lumen, among others. The molecular functions mainly focused on *CXCR* chemokine receptor binding, G protein-coupled receptor binding, and chemokine activity.

There were 11 genes common to drugs and diseases. The biological processes were mainly positive regulation of cell migration involved in sprouting angiogenesis, regulation of wound healing, positive regulation of blood vessel endothelial cell migration, and regulation of coagulation, among others. In order to determine the mechanism of TQHXD against ICH, KEGG enrichment analysis was performed on 11 genes, and it was found that they were mainly involved in fluid shear stress, atherosclerosis, and the HIF-1 signaling pathway.

Molecular docking analysis

In order to analyze the feasibility of TQHXD in the treatment of ICH, molecular docking analysis was performed on the core active ingredients of TQHXD and the key targets of ICH. First, the 4 key genes were imported into STRING (http://stitch.embl.de/) to accurately obtain the PDB numbers of these proteins in humans, and then 2D structures of the 4 components were obtained through PDB numbers. The PDB numbers of the crystal structures of *PTGS1*, *NR3C2*, *ANXA1*, and *VEGF-A* were 6Y3C, 3VHV, 1QLS, and 3QTK, respectively. Molecular docking was

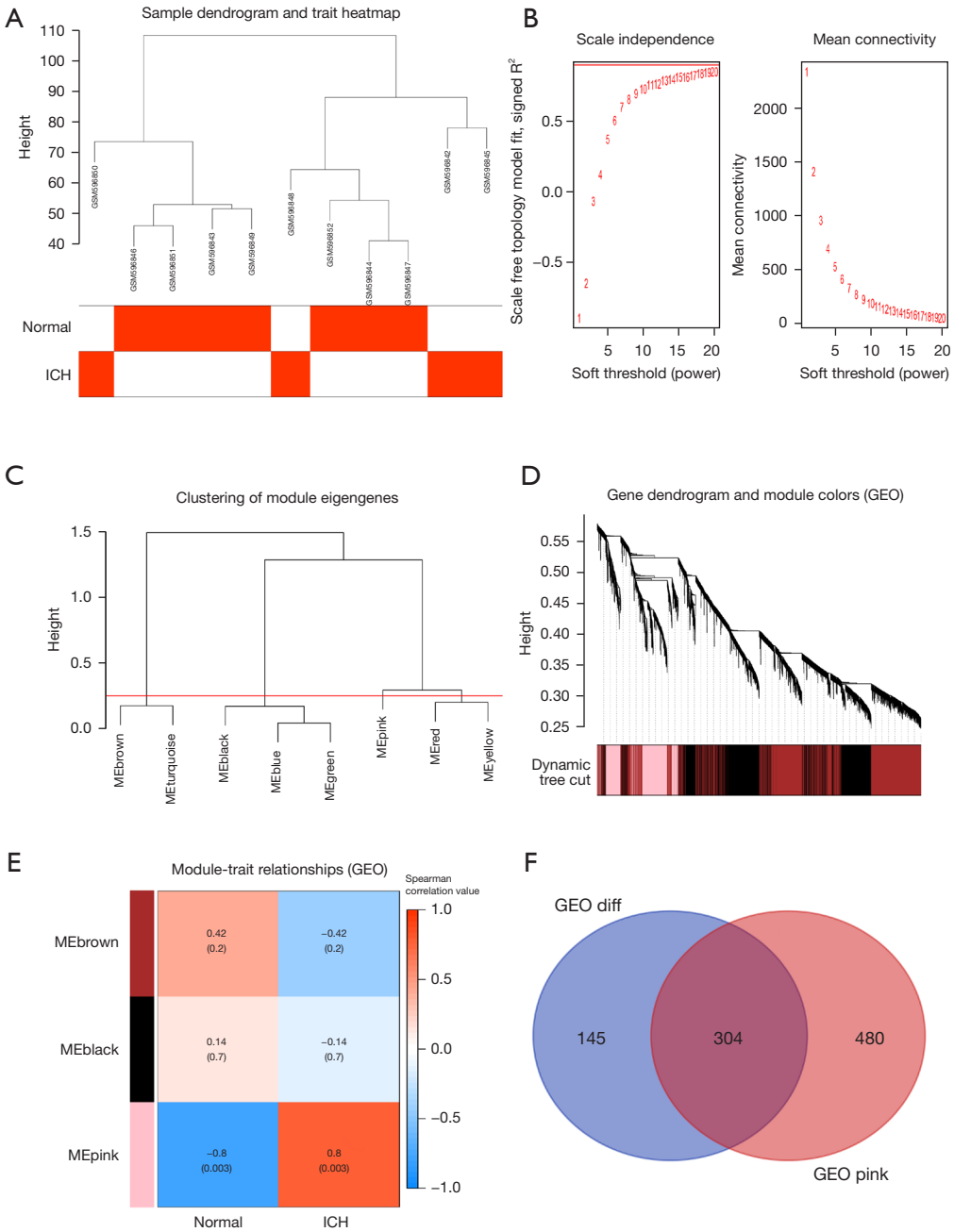

Figure 4 WGCNA selection module and selection of differential co-expressed genes. (A) Outliers were detected in the sample cluster. (B) The cut-off point was set as 0.9, and the soft threshold power was set as β=18. (C) Correlation diagram between modules obtained by clustering according to inter-gene expression levels. (D) Tree diagram of all differentially expressed genes based on the cluster of difference measurement. The colored bands show the results from the automated monolithic analysis. (E) Heat map of the correlation between module characteristic genes and phenotypes. We chose the MEpink module for subsequent analysis (the ordinate value is the correlation coefficient of feature module). (F) The intersection gene of ICH differentially expressed genes and the MEpink module. WGCNA, weighted gene co-expression network analysis; diff, differentially expressed gene.

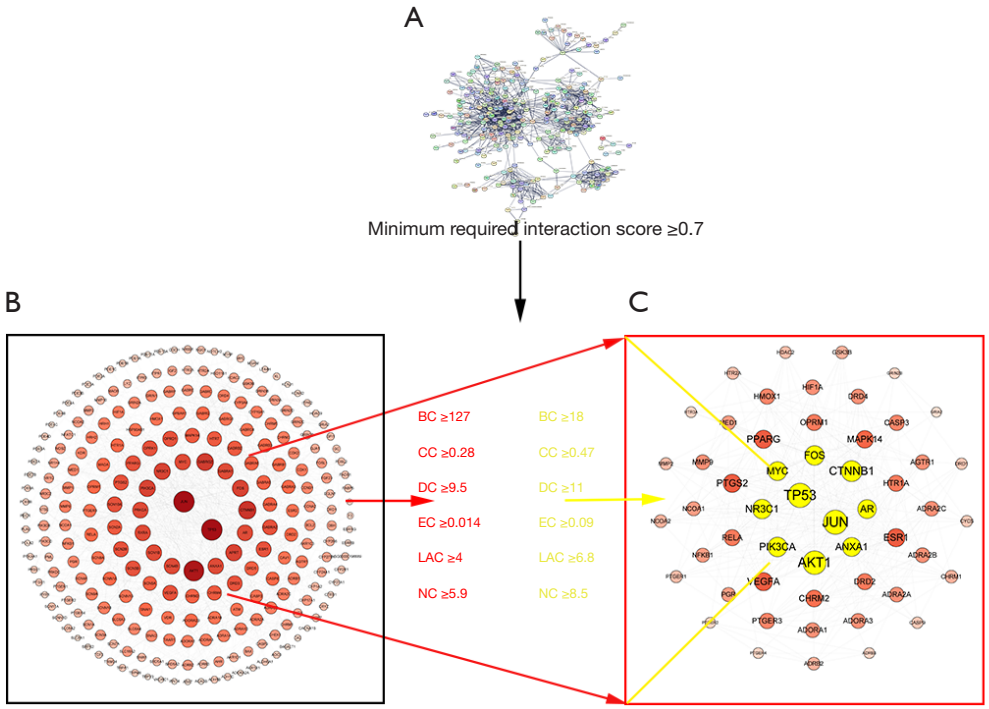

Figure 5 The target core interaction network of effective ingredients in traditional Chinese medicine formulas was determined. (A) The target interaction network of effective ingredients. (B,C) The target core interaction network of effective ingredients in Tongqiao Huoxue formulas. BC, betweenness centrality; CC, closeness centrality; DC, degree centrality; EC, eigenvector centrality; NC, network centrality; LAC, local average connectivity.

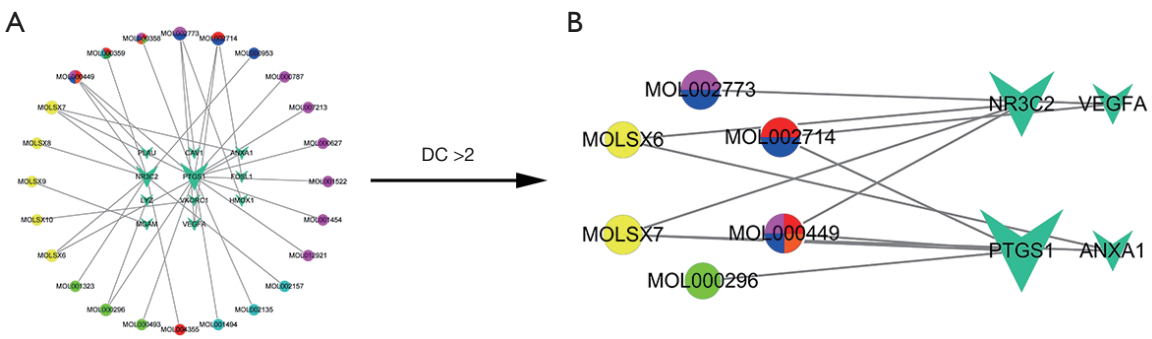

Figure 6 ICH drug-disease-target network for TQHXD therapy. (A) TQHXD-ICH-target network. (B) TQHXD-ICH-target core network. The common targets of drug and disease are represented by the inverted triangles and the drugs are represented by circles (Dazao is pink, Honghua is blue, Chishao is red, Taoren is green, Shexiang is yellow, and Chuanxiong is cyan, and various drugs are indicated by various color combinations). TQHXD, Tongqiao Huoxue Decoction; ICH, intracerebral hemorrhage; DC, degree centrality.

conducted for all the core TCM small molecules and the common disease-drug targets, and the results were shown in a heat map (*Figure 9*). Interestingly, we found that in the 4 lowest binding energies of small molecule drugs and proteins, 2 kinds of small molecules were the main active ingredients of musk, so we showed their docking diagrams with 4 kinds of protein macromolecules in *Figure 10*. The figure shows the binding site and length of the hydrogen bond between the hydrogen bond of the small drug molecule and the protein residue. For example, for Morin's

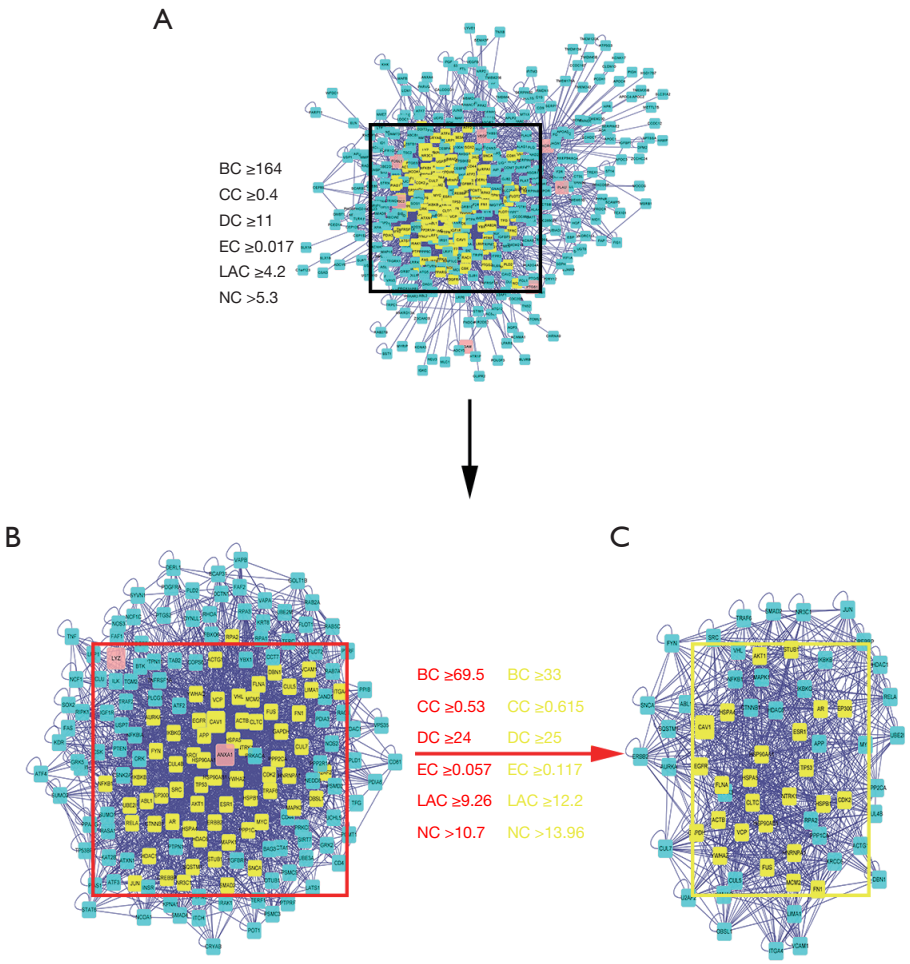

Figure 7 Common PPI network of TQHXD and ICH targets. (A) The PPI network of TQHXD and ICH targets consists of 526 nodes and 4,793 edges. (B) PPI network of significant proteins extracted from (A). The network consists of 178 nodes and 2,517 edges. (C) PPI network of significant proteins in (B). The network consists of 65 nodes and 847 edges. TQHXD, Tongqiao Huoxue Decoction; ICH, intracerebral hemorrhage; BC, betweenness centrality; CC, closeness centrality; DC, degree centrality; EC, eigenvector centrality; NC, network centrality; LAC, local average connectivity; PPI, protein-protein interaction.

ionic bond and *PTGS1* GLN-461 residue, GLY-45 residue, and GLU-465, the residue and ionic bond lengths were 2.4 angstroms, 2.6 angstroms, and 3.0 angstroms, respectively.

TQHXD treatment of ICH-related mechanisms

In order to illustrate the possible mechanism of TQHXD in the treatment of ICH, we performed GO analysis of core genes such as *ANXA1*, *NR3C2*, *PTGS1*, and *VEGF-A* in the CTD network. As shown in *Figure 11A*, these genes were mainly involved in the prostaglandin metabolic process, prostaglandin biosynthetic process, positive regulation of blood vessel endothelial cell migration, and other biological processes. The heat map in *Figure 11B* shows that genes such as ANXA1, PTGS1, and *VEGF-A* were highly expressed in ICH, while *NR3C2* showed low expression in ICH. *Figure 11C* shows the possible mechanism of action of morin, fumarine, baicalein, and other Chinese medicine monomers on target genes for the treatment of ICH. They may mediate anti-inflammatory mechanisms and promote blood vessel regeneration through fluid shear stress, atherosclerosis, and HIF-1 signaling pathways, among other processes.

Discussion

Nervous system diseases are an important cause of disability

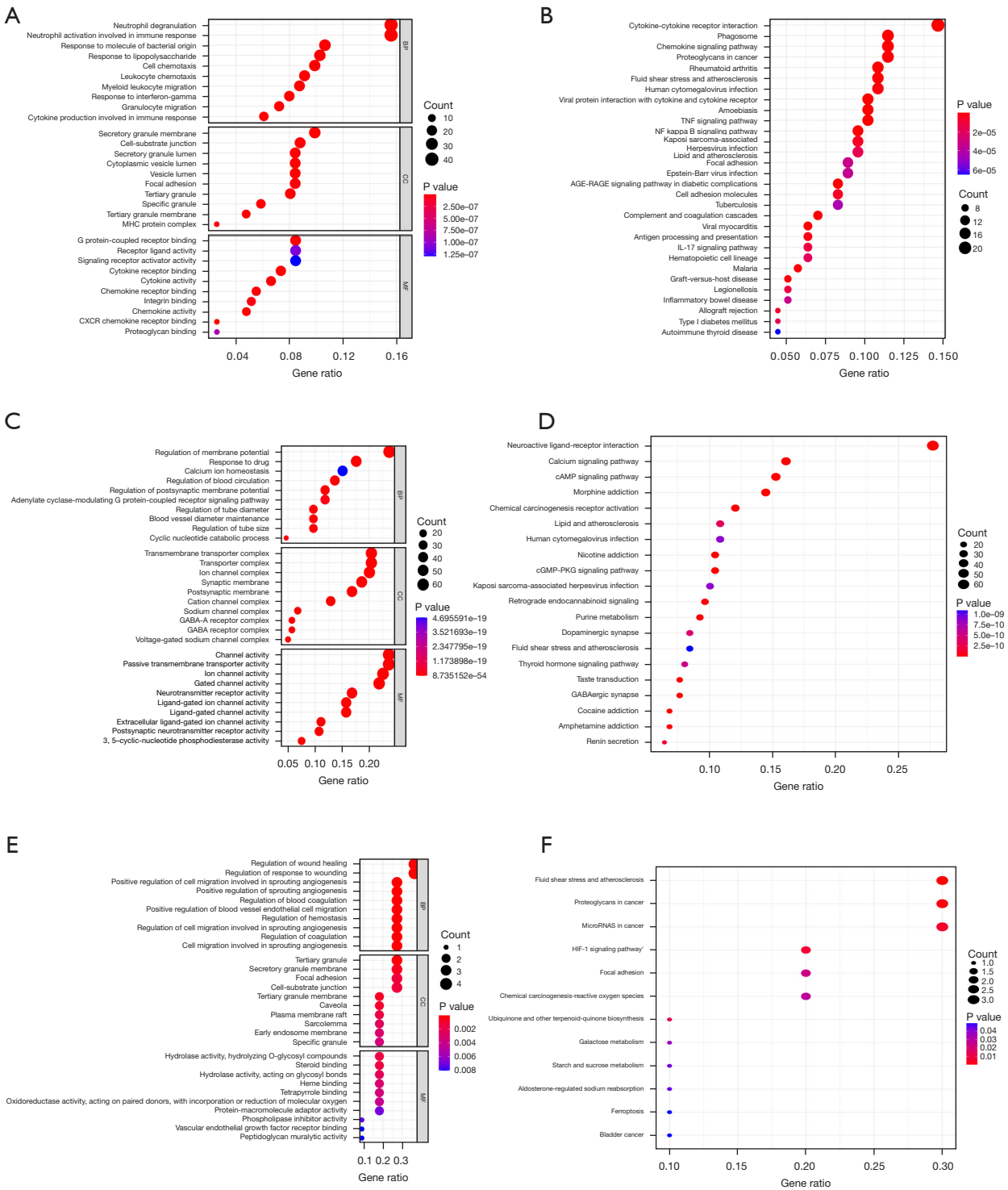

Figure 8 Functional enrichment analysis of TQHXD targets and ICH differential genes. (A,B) GO and KEGG functional enrichment analysis of ICH differential genes. (C,D) GO and KEGG functional enrichment analysis of TQHXD targets. (E,F) GO and KEGG functional enrichment analysis of common targets of TQHXD and ICH. The size of the bubble indicates the number of enriched genes, and the color indicates P value. TQHXD, Tongqiao Huoxue Decoction; ICH, intracerebral hemorrhage; GO, Gene Ontology; KEGG, Kyoto Encyclopedia of Genes and Genomes; BP, biological process; CC, cell components; MF, molecular function.

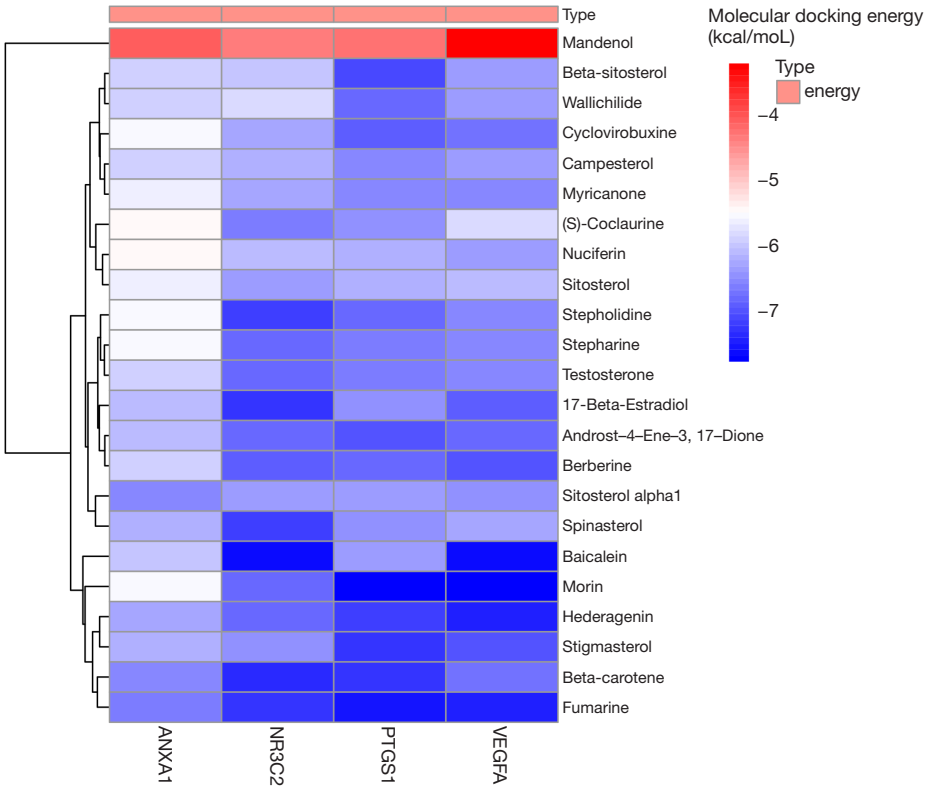

Figure 9 Molecular docking energy heat map. Molecular docking of ANXA1, NR3C2, PTGS1, and VEGFA proteins in *Figure 5B* was performed with the corresponding small molecule drugs in the network, and the docking energy was drawn into a heat map. Red represents high docking energy required, and blue represents low docking energy required, the ordinate value is the energy of docking (Kcal/mol).

and death worldwide. On a global scale, although the mortality rate of stroke and infectious neurological diseases has been greatly reduced, the burden of stroke is likely to continue to increase around the world (1). In recent years, acute clinical interventions (including drug therapy for hematoma enlargement, hemoglobin toxicity, inflammation, edema, anticoagulation reversal, and minimally invasive surgery) for the treatment of ICH have been shown to improve the acute prognosis (33). However, the clinical effect is still poor, and there are still many challenges.

In ancient China, diseases were usually named according to different symptoms. TCM has a wealth of clinical practice experience. From the perspective of clinical symptoms, ICH in Western medicine is similar to stroke in Chinese medicine. Therefore, ICH can be attributed to the category of "stroke". The pathogenesis of stroke in Chinese medicine is caused by the incoordination of yin and yang and the deficiency of both qi and blood. Among them, the principle of treatment of the internal organs for patients with ICH is to remove blood stasis and heat, reduce phlegm, and resuscitation. Blood stasis is the core of ICH.

THXD is based on Wang Qingren's correction of medical errors. It is composed of Shexiang (Moschus), Chishao (Radix Paeoniae Rubra), Chuanxiong (Chuanxiong Rhizoma), Taoren (Persicae Semen), Honghua (Carthami Flos), green onions (Allii Fistulost Bulbus), Dazao (Jujubae Fruale Roscoe), and Shenjang (Zingiber Officinale Roscoe) Composition, they can invigorate blood, remove blood stasis, restore consciousness, and cause resuscitation. The main components of TQHXD in treating traumatic ICH include musk, safflower, ligusticum chuanxiong, peony root and peach kernel. Safflower, ligusticum chuanxiong, peach kernel and so on can dredge blood vessels and reduce brain tissue edema, and can promote angiogenesis and so on. On the other hand, ligusticum chuanxiong promotes nerve regeneration by regulating reactive astrocyte proliferation and maintaining blood-brain barrier. Muscone can reduce the expression of *HIF-1A*, resulting in decreased expression

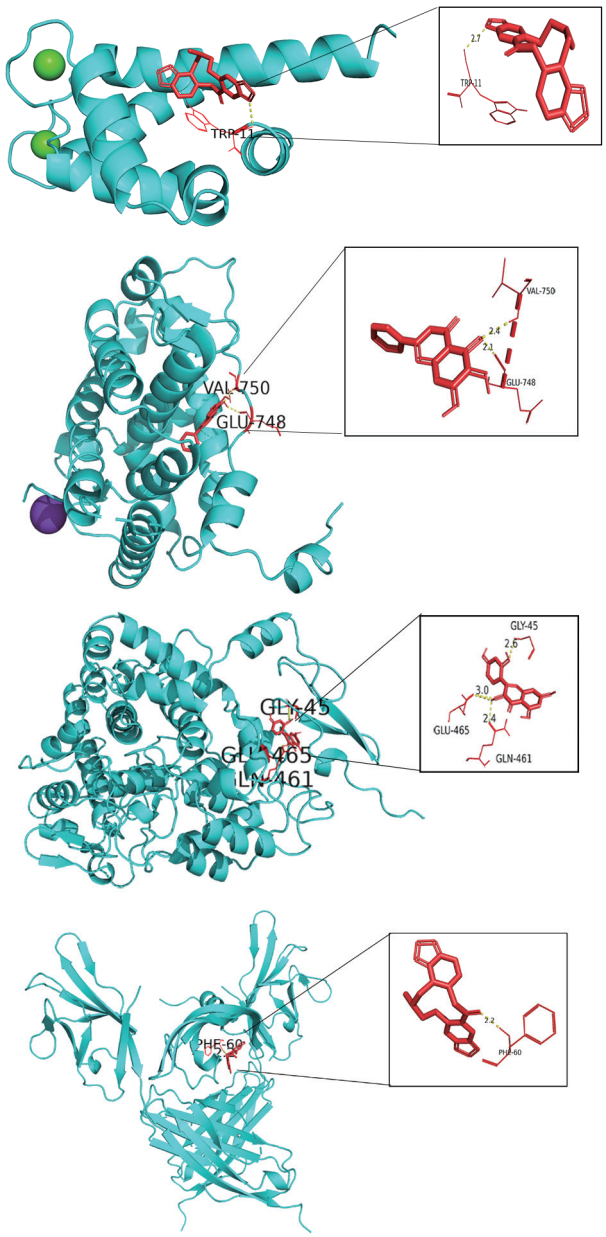

Figure 10 Core protein docking with small molecules. The molecules and drugs with the lowest docking energies are visualized in *Figure 9*, namely ANXA1 and fumarine, NR3C2 and baicalein, PTGS1 and morin, and VEGFA and fumarine. Small molecule drugs and interacting amino acids are red, proteins are blue, their interactions are yellow dotted lines, and numbers are bond lengths.

of MMPs, aquaporin-4 (*AQP-4*), and *VEGF*, thereby changing the permeability of BBB, promoting hematoma absorption, and restoring neural function (34-36).

Musk is the secretion of male musk deer and is one of the most important components of TQHXD. Musk can pass the BBB, and its polypeptide glycoproteins may have anti-inflammatory effects. Its unique aroma is often used in resuscitation drugs. It can resuscitate consciousness and relieve pain, and has been documented in Shennong Herbology. A total of 29 compounds were found in the BATMAN-TCM analysis platform, including muscone, muscopyridine, estradiol, androgen, and morin (37). In a rat model of cerebral ischemia, muscone and medicines such as ligustilide and hydroxysafflor yellow A could up-regulate the expression of ZO-1, occludin, and claudin-5 and down-regulate aquaporin-4 (AQP-4) (38). On the other hand, the results of musk and other drugs in an animal model of cerebral hemorrhage showed that treatment with TCM and acupuncture could improve neurological dysfunction (39). Muscone is one of the main components of musk. Muscone was found to inhibit glutamate-induced death of PC12 cells and cortical neuronal apoptosis by cell viability determination and gas chromatography-mass spectrometry (40). Muscone improved synaptic dysfunction and cognitive deficits in APP/PS1 mice (41). Furthermore, muscone treatment could alleviate memory dysfunction in APP/PS1 mice, reduce Aβ levels, and enhance synaptic plasticity (42). Musk ketone molecules are responsible for the main physiological activity of musk, which can not only resist dementia and fight against cerebral ischemia, but also has low cytotoxicity and a variety of potential health benefits, such as anti-tumor effects, beneficial effects on ischemic heart disease, and the inhibition of diabetic peripheral neuropathy (38,43,44). These effects will help promote cell proliferation and angiogenesis, reduce apoptosis and inflammation, and maintain cell viability, among others.

Radix Paeoniae Rubra (RPR) is used as a prescription for miscellaneous diseases caused by colds by Zhang Zhongjing. RPR can protect the liver by inhibiting inflammation, resisting oxidative damage, and scavenging free radicals (45). Paeoniae, ethyl palmitate, and ethyl linoleate are 3 major hepatoprotective active components in RPR (46). Experimental results showed that Radix Paeoniae could protect against ischemia/reperfusion (I/R) by inhibiting I/R-induced neutrophil infiltration and pro-inflammatory cytokine production (I/R) induced hepatocytes and inhibited hepatocyte apoptosis (47). Radix Paeoniae Rubra can inhibit neuronal apoptosis by reducing the apoptotic signal dependent on endoplasmic reticulum (ER) stress and protecting the BBB (48). The active ingredients ethyl palmitic acid and linoleic acid ethyl ester

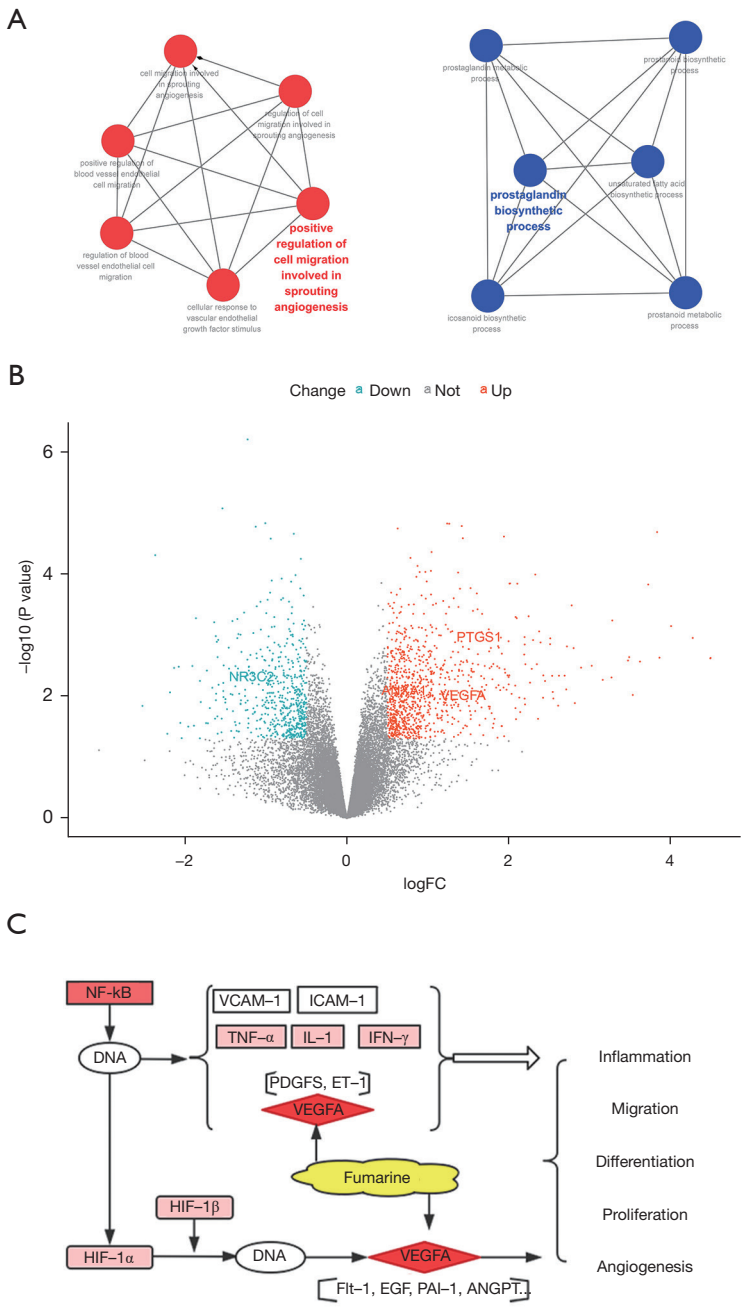

Figure 11 Related mechanisms of TQHXD therapy for ICH. (A) Molecular docking core protein GO analysis. (B) Molecular docking core protein DEGs volcano plot in ICH. (C) Combined with *Figure 8F*, the core protein VEGFA of TQHXD can treat ICH-related mechanisms through the HIF-1 signaling pathway. TQHXD, Tongqiao Huoxue Decoction; ICH, intracerebral hemorrhage; GO, Gene Ontology; DEGs, differentially expressed genes; FC, fold change.

demonstrate certain anti-inflammatory and antioxidant effects. Hexadecenoic acid ethyl ester is an inhibitor of inflammatory cells, mainly by reducing neutrophil infiltration, as determined by myeloperoxidase (MPO) activity, leading to inflammatory exudate of prostaglandin E2 (PGE2) levels, which can reduce Edema of the soles of the feet in rats (49). Overall, these results suggest that RPR can inhibit the toxic and side effects of inflammatory factors

and oxygen free radicals on the body and organs and reduce tissue edema, which may play a certain role in inflammatory exudation and the increase of oxygen free radicals in the acute phase of ICH.

Zingiber Officinale Roscoe is the rhizome of the ginger family turmeric, which has been used as a food, spice, tonic, and flavoring agent, as well as a traditional medicine. It mainly includes terpenes, polysaccharides, phenolic compounds, lipids, organic acids, and other important substances (50,51). The reason why ginger has a therapeutic effect on diseases is mainly due to its phenolic compounds, such as gingerol and zingerone (52-54). These biologically active ingredients mainly act as antioxidants, anti-inflammatory agents, anti-microbial agents, anti-cancer agents, neuroprotective agents, cardiovascular protective agents, respiratory protective agents, weight loss drugs, anti-diabetics, anti-nausea agents, and antiemetics. Ginger components are involved in biological activities (55) such as immunology and inflammation, apoptosis, cell cycle/DNA damage, chromatin/epigenetic regulation, cytoskeleton regulation and adhesion, and nerve cell activity. Then, through autophagy, cell metabolism, promote signal pathways such as mitogen-activated protein kinases play a role in relation to cell functions/mechanisms (56).

The main bioactive components of Carthami Flos are hydroxysafflor yellow A and total flavonoids. In animal models of acute lung injury, Carthami Flos can significantly reduce the infiltration of activated neutrophils by reducing the levels of TNF-α and IL-6, thus protecting mice from lipopolysaccharide (LPS)-induced acute lung injury (57). Hongthuan injection can prevent I/R injury, improve hemodynamics, reduce the generation of free radicals, and increase the production of nitric oxide (NO). Carthami Flos has been used for the treatment of cerebral ischemia, cerebral hemorrhage, vertebrobasilar ischemic vertigo, cerebral infarction, coronary heart disease, heart failure, diabetic complications, and primary dysmenorrhea (58).

Rhizoma Chuanxiong has the effects of promoting blood circulation, removing blood stasis, dispelling wind, and relieving pain. Experimental evidence shows that Rhizoma Chuanxiong may exert neuroprotective effects by inhibiting calcium overload and inhibiting anti-inflammatory responses (59,60). There is also evidence that treatment with Rhizoma Chuanxiong can reduce the cognitive function and motor protection in a rat model of traumatic brain injury (TBI), reduce BBB leakage and brain edema, reduce neuron loss, activate microglia and astrocytes, and increase the proliferation of neural stem cells (61). A study has shown that the neuroprotection provided by Rhizoma Chuanxiong is due to the pro-apoptotic and anti-apoptotic biomarkers of Bcl-2 and cleaved caspase-3, BDNF, MCP-1, Hcy, and other multiple pathways that jointly trigger mitochondrial-associated Bax/activation of Bcl-2 and caspase-3 apoptotic pathways (62). These a previous study indicate that Rhizoma Chuanxiong is expected to be a promising neuroprotective agent.

Prostaglandin (PTG) is involved in normal homeostasis and inflammation. The main physiological effects of PTG include vasodilation and vascular leakage (*PTGE2*) (63). COX enzyme inhibitors such as NSAIDs are widely used in the treatment of pain, inflammation, fever, and colon cancer (64). A study has shown that sildenafil can improve the vasodilation function of acetylcholine, enhancing the bioavailability of NO, reducing oxidative stress and COX-1 prostaglandins, and improving cGMP/PKG signal transduction, thereby reversing endothelial dysfunction in spontaneously hypertensive rats (SHR) (65). In addition, sildenafil can reduce structural endothelial damage. Therefore, the up-regulated expression of the PTGS1 gene in ICH tissue indicates that TQHXD can prevent the elevation of blood pressure and is conducive to the early antihypertensive treatment of ICH.

NR3C2 is a mineralocorticoid receptor gene. A study using Sanger sequencing technology to analyze the *NR3C2* gene in 450 gestational hypertension (GH) patients and 450 healthy controls found that the gene-gene interaction at rs5522, rs2070951, and rs5534 affected the risk of GH (OR =1.34, 95% CI: 1.12–1.64, P<0.001) (66). In addition, the rs2070951 single nucleotide polymorphism of NR3C2 regulates multiple memory systems through cortisol (67). It was found in animal models of cognitive impairment after stroke that the up-regulation of miR-135b-5p can reduce neuronal damage and inflammation in post-stroke cognitive impairment (PSCI) by targeting *NR3C2* (68). This may be beneficial to the recovery of neuronal damage in the later stage of ICH and speeds up the recovery time of patients.

Annexin A1 (*ANXA1*) is an important member of the annexin family of Ca^{2+}-dependent phospholipid binding proteins (69). In a preclinical model of inflammatory disease, the stimulation of FPR2 by *ANXA1* reduced inflammation and immune cell activation (70). In the tissues surrounding the hematoma of ICH patients, high-throughput sequencing found that among all the anti-inflammatory factors, *ANXA1* was most obviously induced, indicating that it is an endogenous protective mechanism (71). Animal experiments have also shown that *ANXA1* can effectively reduce brain edema after

ICH, improve short-term neurological function, improve microglial activation, and improve memory function (72). *ANXA1* plays an important role in neuroinflammation caused by ICH and is also expected to become a therapeutic target.

VEGF receptors belong to the family of receptor tyrosine kinases (73). *VEGF-A* has a variety of protective effects, including promoting angiogenesis, neurogenesis, and neuroprotection, thereby improving functional recovery (74). On the other hand, overexpression of *VEGF-A* increases neurogenesis in mouse brain tissues and induces newly formed neurons to migrate to the peri-infarct cortex (75). In the normal brain, the use of *VEGF-A* can lead to the up-regulation of *VEGFR-1* and *VEGFR-2*, and can significantly increase the formation of cerebral blood vessels (76). Therefore, *VEGF-A* can act as a regulator of neuroprotection and neurogenesis and promote angiogenesis in brain tissue, which is conducive to the recovery of ICH.

ICH is mostly caused by cerebral parenchymal hemorrhage due to hypertension, which presents complex pathophysiological manifestations, including excitotoxicity, increased BBB vascular permeability, inflammation, and oxidative stress, ultimately leading to cell death. If blood pressure is controlled in time, intracranial pressure is actively reduced, cerebral edema is controlled, inflammation is eliminated, new angiogenesis is promoted, and the nerves surrounding edema are protected, the treatment effect and prognosis will be improved. Inflammation is one of the key factors of secondary brain damage caused by ICH. Activated microglia and infiltrating white blood cells have been considered to be important factors in the neuroinflammatory response that promotes disease progression (77). Therefore, anti-inflammatory drugs are expected to reduce brain edema and microglial activation, and play a role in accelerating ICH recovery.

In this study, we analyzed the main bioactive components and pharmacological mechanisms of TQHXD for the treatment of ICH by integrating bioinformatics and network pharmacology. The application of network pharmacology lays the foundation for further study of the mechanism of TQHXD, provides a theoretical basis for systematic experimental study and the clinical application of TQHXD in the treatment of ICH, and provides a new research idea and method for the study of TCM compound therapy for ICH, in particular TQHXD and its associated drug targets. In addition, molecular docking further proved the feasibility of TQHXD in the treatment of ICH. However, the active components and targets of some Chinese medicines have not been fully determined and need to be further confirmed by experiments.

Conclusions

Through network pharmacology, we found that musk, Radix Paeoniae Rubra, Carthami Flos, and other effective active natural ingredients in TQHXD, as well as *PTGS1*, *NR3C2*, *ANXA1*, *VEGF-A*, and other gene targets, can help reduce brain inflammation, improve brain edema, and protect nerves. This provides a basis for drug research and development for the treatment of ICH in the later stage.

Acknowledgments

Funding: None.

Footnote

Reporting Checklist: The authors have completed the STREGA reporting checklist. Available at https://atm.amegroups.com/article/view/10.21037/atm-22-1403/rc

Conflicts of Interest: All authors have completed the ICMJE uniform disclosure form (available at https://atm.amegroups.com/article/view/10.21037/atm-22-1403/coif). The authors have no conflicts of interest to declare.

Ethical Statement: The authors are accountable for all aspects of the work in ensuring that questions related to the accuracy or integrity of any part of the work are appropriately investigated and resolved. The study was conducted in accordance with the Declaration of Helsinki (as revised in 2013).

References

1. GBD 2019 Stroke Collaborators. Global, regional, and national burden of stroke and its risk factors, 1990-2019: a

systematic analysis for the Global Burden of Disease Study 2019. Lancet Neurol 2021;20:795-820.
2. Nobleza COS. Intracerebral Hemorrhage. Continuum (Minneap Minn) 2021;27:1246-77.
3. Gustavsson A, Svensson M, Jacobi F, et al. Cost of disorders of the brain in Europe 2010. Eur Neuropsychopharmacol 2011;21:718-79.
4. Poon MT, Fonville AF, Al-Shahi Salman R. Long-term prognosis after intracerebral haemorrhage: systematic review and meta-analysis. J Neurol Neurosurg Psychiatry 2014;85:660-7.
5. Duan X, Wen Z, Shen H, et al. Intracerebral Hemorrhage, Oxidative Stress, and Antioxidant Therapy. Oxid Med Cell Longev 2016;2016:1203285.
6. Menon G, Johnson SE, Hegde A, et al. Neutrophil to lymphocyte ratio - A novel prognostic marker following spontaneous intracerebral haemorrhage. Clin Neurol Neurosurg 2021;200:106339.
7. Stokum JA, Cannarsa GJ, Wessell AP, et al. When the Blood Hits Your Brain: The Neurotoxicity of Extravasated Blood. Int J Mol Sci 2021;22:5132.
8. Sun Q, Xu X, Wang T, et al. Neurovascular Units and Neural-Glia Networks in Intracerebral Hemorrhage: from Mechanisms to Translation. Transl Stroke Res 2021;12:447-60.
9. Williams-Johnson JA, McDonald AH, Strachan GG, et al. Effects of tranexamic acid on death, vascular occlusive events, and blood transfusion in trauma patients with significant haemorrhage (CRASH-2) A randomised, placebo-controlled trial. West Indian Med J 2010;59:612-24.
10. Hemphill JC 3rd, Greenberg SM, Anderson CS, et al. Guidelines for the Management of Spontaneous Intracerebral Hemorrhage: A Guideline for Healthcare Professionals From the American Heart Association/ American Stroke Association. Stroke 2015;46:2032-60.
11. Xu S, Pang Q, Lin Z, et al. Effect of integrated traditional Chinese and Western medicine therapy for acute hypertensive intracerebral hemorrhage: a meta-analysis. Artif Cells Nanomed Biotechnol 2017;45:1-6.
12. Liu C, Zhou L, Shui Z. Tongqiao huoxue tang and buyang huanwu tang for treatment of vascular dementia--a report of 36 cases. J Tradit Chin Med 2003;23:243-5.
13. Wang N, Deng Y, Wei W, et al. Serum containing Tongqiaohuoxue decoction suppresses glutamate-induced PC12 cell injury. Neural Regen Res 2012;7:1125-31.
14. Kim SH, Park HS, Hong MJ, et al. Tongqiaohuoxue decoction ameliorates obesity-induced inflammation and the prothrombotic state by regulating adiponectin and plasminogen activator inhibitor-1. J Ethnopharmacol 2016;192:201-9.
15. Li L, Wang N, Jin Q, et al. Protection of Tong-Qiao-Huo-Xue Decoction against Cerebral Ischemic Injury through Reduction Blood-Brain Barrier Permeability. Chem Pharm Bull (Tokyo) 2017;65:1004-10.
16. Ru J, Li P, Wang J, et al. TCMSP: a database of systems pharmacology for drug discovery from herbal medicines. J Cheminform 2014;6:13.
17. Liu Z, Guo F, Wang Y, et al. BATMAN-TCM: a Bioinformatics Analysis Tool for Molecular mechANism of Traditional Chinese Medicine. Sci Rep 2016;6:21146.
18. Wang Y, Zheng C, Huang C, et al. Systems Pharmacology Dissecting Holistic Medicine for Treatment of Complex Diseases: An Example Using Cardiocerebrovascular Diseases Treated by TCM. Evid Based Complement Alternat Med 2015;2015:980190.
19. Perlman L, Gottlieb A, Atias N, et al. Combining drug and gene similarity measures for drug-target elucidation. J Comput Biol 2011;18:133-45.
20. Wang Y, Bryant SH, Cheng T, et al. PubChem BioAssay: 2017 update. Nucleic Acids Res 2017;45:D955-63.
21. UniProt Consortium. UniProt: the universal protein knowledgebase in 2021. Nucleic Acids Res 2021;49:D480-9.
22. Barrett T, Wilhite SE, Ledoux P, et al. NCBI GEO: archive for functional genomics data sets--update. Nucleic Acids Res 2013;41:D991-5.
23. Zhang B, Horvath S. A general framework for weighted gene co-expression network analysis. Stat Appl Genet Mol Biol 2005;4:Article17.
24. Langfelder P, Horvath S. WGCNA: an R package for weighted correlation network analysis. BMC Bioinformatics 2008;9:559.
25. Szklarczyk D, Gable AL, Lyon D, et al. STRING v11: protein-protein association networks with increased coverage, supporting functional discovery in genome-wide experimental datasets. Nucleic Acids Res 2019;47:D607-13.
26. Martin A, Ochagavia ME, Rabasa LC, et al. BisoGenet: a new tool for gene network building, visualization and analysis. BMC Bioinformatics 2010;11:91.
27. Tang Y, Li M, Wang J, et al. CytoNCA: a cytoscape plugin for centrality analysis and evaluation of protein interaction networks. Biosystems 2015;127:67-72.
28. Muthiah A, Keller SR, Lee JK. Module Anchored Network Inference: A Sequential Module-Based Approach to Novel

Gene Network Construction from Genomic Expression Data on Human Disease Mechanism. Int J Genomics 2017;2017:8514071.
29. Berman HM, Westbrook J, Feng Z, et al. The Protein Data Bank. Nucleic Acids Res 2000;28:235-42.
30. Wang Y, Xiao J, Suzek TO, et al. PubChem's BioAssay Database. Nucleic Acids Res 2012;40:D400-12.
31. Forli S, Huey R, Pique ME, et al. Computational protein-ligand docking and virtual drug screening with the AutoDock suite. Nat Protoc 2016;11:905-19.
32. Vilar S, Cozza G, Moro S. Medicinal chemistry and the molecular operating environment (MOE): application of QSAR and molecular docking to drug discovery. Curr Top Med Chem 2008;8:1555-72.
33. Hostettler IC, Seiffge DJ, Werring DJ. Intracerebral hemorrhage: an update on diagnosis and treatment. Expert Rev Neurother 2019;19:679-94.
34. Wang GY, Wang N, Liao HN. Effects of Muscone on the Expression of P-gp, MMP-9 on Blood-Brain Barrier Model In Vitro. Cell Mol Neurobiol 2015;35:1105-15.
35. Yu B, Yao Y, Zhang X, et al. Synergic Neuroprotection Between Ligusticum Chuanxiong Hort and Borneol Against Ischemic Stroke by Neurogenesis via Modulating Reactive Astrogliosis and Maintaining the Blood-Brain Barrier. Front Pharmacol 2021;12:666790.
36. Zhang Q, Zhang L, Liu Y, et al. Research progress on the pharmacological effect and clinical application of Tongqiao Huoxue Decoction in the treatment of ischaemic stroke. Biomed Pharmacother 2021;138:111460.
37. Lv S, Lei Z, Yan G, et al. Chemical compositions and pharmacological activities of natural musk (Moschus) and artificial musk: A review. J Ethnopharmacol 2022;284:114799.
38. Yang LQ, Yu SP, Yang YT, et al. Muscone derivative ZM-32 inhibits breast tumor angiogenesis by suppressing HuR-mediated VEGF and MMP9 expression. Biomed Pharmacother 2021;136:111265.
39. Chen JC. The effects of acupuncture and traditional Chinese medicines on apoptosis of brain tissue in a rat intracerebral hemorrhage model. Physiol Behav 2015;151:421-5.
40. Wei G, Chen DF, Lai XP, et al. Muscone exerts neuroprotection in an experimental model of stroke via inhibition of the fas pathway. Nat Prod Commun 2012;7:1069-74.
41. Mayor D, Tymianski M. Neurotransmitters in the mediation of cerebral ischemic injury. Neuropharmacology 2018;134:178-88.
42. Liu Y, Bian H, Xu S, et al. Muscone Ameliorates Synaptic Dysfunction and Cognitive Deficits in APP/PS1 Mice. J Alzheimers Dis 2020;76:491-504.
43. Wang X, Meng H, Chen P, et al. Beneficial effects of muscone on cardiac remodeling in a mouse model of myocardial infarction. Int J Mol Med 2014;34:103-11.
44. Dong J, Li H, Bai Y, et al. Muscone ameliorates diabetic peripheral neuropathy through activating AKT/mTOR signalling pathway. J Pharm Pharmacol 2019;71:1706-13.
45. Wang R, Xiong AZ, Teng ZQ, et al. Radix Paeoniae Rubra and Radix Paeoniae Alba Attenuate CCl4-induced acute liver injury: an ultra-performance liquid chromatography-mass spectrometry (UPLC-MS) based metabolomic approach for the pharmacodynamic study of Traditional Chinese Medicines (TCMs). Int J Mol Sci 2012;13:14634-47.
46. Jiang H, Li J, Wang L, et al. Total glucosides of paeony: A review of its phytochemistry, role in autoimmune diseases, and mechanisms of action. J Ethnopharmacol 2020;258:112913.
47. Jiang ZQ, Yan XJ, Bi L, et al. Mechanism for hepato-protective action of Liangxue Huayu Recipe (LHR): blockade of mitochondrial cytochrome c release and caspase activation. J Ethnopharmacol 2013;148:851-60.
48. Gu J, Chen J, Yang N, et al. Combination of Ligusticum chuanxiong and Radix Paeoniae ameliorate focal cerebral ischemic in MCAO rats via endoplasmic reticulum stress-dependent apoptotic signaling pathway. J Ethnopharmacol 2016;187:313-24.
49. Saeed NM, El-Demerdash E, Abdel-Rahman HM, et al. Anti-inflammatory activity of methyl palmitate and ethyl palmitate in different experimental rat models. Toxicol Appl Pharmacol 2012;264:84-93.
50. Ali BH, Blunden G, Tanira MO, et al. Some phytochemical, pharmacological and toxicological properties of ginger (Zingiber officinale Roscoe): a review of recent research. Food Chem Toxicol 2008;46:409-20.
51. Govindarajan VS. Ginger--chemistry, technology, and quality evaluation: part 1. Crit Rev Food Sci Nutr 1982;17:1-96.
52. Mohd Yusof YA. Gingerol and Its Role in Chronic Diseases. Adv Exp Med Biol 2016;929:177-207.
53. Ahmad B, Rehman MU, Amin I, et al. A Review on Pharmacological Properties of Zingerone (4-(4-Hydroxy-3-methoxyphenyl)-2-butanone). ScientificWorldJournal 2015;2015:816364.
54. Wang S, Zhang C, Yang G, et al. Biological properties of 6-gingerol: a brief review. Nat Prod Commun

2014;9:1027-30.
55. Mao QQ, Xu XY, Cao SY, et al. Bioactive Compounds and Bioactivities of Ginger (Zingiber officinale Roscoe). Foods 2019;8:185.
56. Kiyama R. Nutritional implications of ginger: chemistry, biological activities and signaling pathways. J Nutr Biochem 2020;86:108486.
57. Wan LM, Tan L, Wang ZR, et al. Preventive and therapeutic effects of Danhong injection on lipopolysaccharide induced acute lung injury in mice. J Ethnopharmacol 2013;149:352-9.
58. Feng X, Li Y, Wang Y, et al. Danhong injection in cardiovascular and cerebrovascular diseases: Pharmacological actions, molecular mechanisms, and therapeutic potential. Pharmacol Res 2019;139:62-75.
59. Wang M, Yao M, Liu J, et al. Ligusticum chuanxiong exerts neuroprotection by promoting adult neurogenesis and inhibiting inflammation in the hippocampus of ME cerebral ischemia rats. J Ethnopharmacol 2020;249:112385.
60. Qian W, Xiong X, Fang Z, et al. Protective effect of tetramethylpyrazine on myocardial ischemia-reperfusion injury. Evid Based Complement Alternat Med 2014;2014:107501.
61. Liu ZK, Ng CF, Shiu HT, et al. Neuroprotective effect of Da Chuanxiong Formula against cognitive and motor deficits in a rat controlled cortical impact model of traumatic brain injury. J Ethnopharmacol 2018;217:11-22.
62. Zhao T, Fu Y, Sun H, et al. Ligustrazine suppresses neuron apoptosis via the Bax/Bcl-2 and caspase-3 pathway in PC12 cells and in rats with vascular dementia. IUBMB Life 2018;70:60-70.
63. Cornejo-García JA, Perkins JR, Jurado-Escobar R, et al. Pharmacogenomics of Prostaglandin and Leukotriene Receptors. Front Pharmacol 2016;7:316.
64. Agúndez JA, Blanca M, Cornejo-García JA, et al. Pharmacogenomics of cyclooxygenases. Pharmacogenomics 2015;16:501-22.
65. Leal MAS, Aires R, Pandolfi T, et al. Sildenafil reduces aortic endothelial dysfunction and structural damage in spontaneously hypertensive rats: Role of NO, NADPH and COX-1 pathways. Vascul Pharmacol 2020;124:106601.
66. Cui Z, Xu J, Jiang W. NR3C2 gene polymorphism is associated with risk of gestational hypertension in Han Chinese women. Medicine (Baltimore) 2019;98:e18215.
67. Langer K, Moser D, Otto T, et al. Cortisol modulates the engagement of multiple memory systems: Exploration of a common NR3C2 polymorphism. Psychoneuroendocrinology 2019;107:133-40.
68. Huang Y, Wang Y, Ouyang Y. Elevated microRNA-135b-5p relieves neuronal injury and inflammation in post-stroke cognitive impairment by targeting NR3C2. Int J Neurosci 2022;132:58-66.
69. Gerke V, Creutz CE, Moss SE. Annexins: linking Ca2+ signalling to membrane dynamics. Nat Rev Mol Cell Biol 2005;6:449-61.
70. Bena S, Brancaleone V, Wang JM, et al. Annexin A1 interaction with the FPR2/ALX receptor: identification of distinct domains and downstream associated signaling. J Biol Chem 2012;287:24690-7.
71. Carmichael ST, Vespa PM, Saver JL, et al. Genomic profiles of damage and protection in human intracerebral hemorrhage. J Cereb Blood Flow Metab 2008;28:1860-75.
72. Ding Y, Flores J, Klebe D, et al. Annexin A1 attenuates neuroinflammation through FPR2/p38/COX-2 pathway after intracerebral hemorrhage in male mice. J Neurosci Res 2020;98:168-78.
73. Grassot J, Gouy M, Perrière G, et al. Origin and molecular evolution of receptor tyrosine kinases with immunoglobulin-like domains. Mol Biol Evol 2006;23:1232-41.
74. Thau-Zuchman O, Shohami E, Alexandrovich AG, et al. Vascular endothelial growth factor increases neurogenesis after traumatic brain injury. J Cereb Blood Flow Metab 2010;30:1008-16.
75. Wang Y, Jin K, Mao XO, et al. VEGF-overexpressing transgenic mice show enhanced post-ischemic neurogenesis and neuromigration. J Neurosci Res 2007;85:740-7.
76. Krum JM, Mani N, Rosenstein JM. Angiogenic and astroglial responses to vascular endothelial growth factor administration in adult rat brain. Neuroscience 2002;110:589-604.
77. Aronowski J, Zhao X. Molecular pathophysiology of cerebral hemorrhage: secondary brain injury. Stroke 2011;42:1781-6.

(English Language Editor: C. Betlazar-Maseh)

Cite this article as: Wu J, Li XY, Liang J, Xie J, Deng CN, Chen ZJ, Lai CS, Yang ZJ. Network pharmacological analysis of active components of Tongqiao Huoxue Decoction in the treatment of intracerebral hemorrhage. Ann Transl Med 2022;10(10):567. doi: 10.21037/atm-22-1403